EXPERIMENTAL CYCLIC TESTS AND RETROFIT OF RC HOLLOW PIERS

Pedro DELGADO[1], Patrício ROCHA[2], Vitorino RODRIGUES[3], Miguel SANTOS[4], António ARÊDE[5], Nelson VILA POUCA[6], Anibal COSTA[7] and Raimundo DELGADO[8]

SUMMARY

The main purpose of this paper is to present an experimental campaign of reinforced concrete hollow section piers with different cross sections under cyclic loading, comparing the obtained results with those obtained for the same piers after seismic retrofitting, and evaluating benefits concerning their structural behaviour. The setup of the RC pier experimental tests was designed to carry out cyclic horizontal top displacements with axial load using two orthogonal actuators with a sliding device to allow pier top displacements and rotations, in spite of the vertical actuator being fixed to a steel portal frame. Representative of typical bridge construction, square and rectangular hollow section RC piers were tested at LESE – the Laboratory of Earthquake and Structural Engineering at Faculty of Engineering of University of Porto. The structural behaviour and safety improvement of these piers are presented, with the retrofit techniques adopted, as well as the illustration of the external and internal damage pattern. The framework of this study is, therefore, to develop and calibrate procedures enabling the evaluation of the different retrofit solution efficiency, their possibilities and fields of application.

1. INTRODUCTION

Bridges and viaducts are amongst all the structures, those that sustain the most damage, as clearly demonstrated in several reports of recent earthquakes. Even for "moderate magnitude" earthquakes, the consequences in these structures have been very dramatic, in many occasions causing their partial destruction, and in some cases total collapse, with corresponding heavy costs. In comparative terms, these consequences of bridge vulnerability are found greater than those observed in building structures and, in most cases, the bridge safety is limited and conditioned by pier capacities. Several studies and works have been carried out on solid piers and can be applied to building structures; however, for hollow piers much less research is found in the literature.

---

[1] Polytechnic Institute - Apartado 574, 4901-908 Viana do Castelo, Portugal
Email : pdelgado@estg.ipvc.pt

[2] Polytechnic Institute - Apartado 574, 4901-908 Viana do Castelo, Portugal
Email : procha@estg.ipvc.pt

[3] Porto University - Faculty of Engineering, Rua Dr. Roberto Frias, s/n 4200-465 Porto, Portugal
Email : vidigal.rodrigues@fe.up.pt

[4] S.T.A.P. – Reparação, consolidação e modificação de estruturas, S. A., Porto, Portugal
Web pag : www.stap.pt

[5] Porto University - Faculty of Engineering, Rua Dr. Roberto Frias, s/n 4200-465 Porto, Portugal
Email : aarede@fe.up.pt

[6] Porto University - Faculty of Engineering, Rua Dr. Roberto Frias, s/n 4200-465 Porto, Portugal
Email : nelsonvp@fe.up.pt

[7] Universidade de Aveiro, Campus Universitário de Santiago, 3810-193 Aveiro, Portugal
Email : acosta@civil.ua.pt

[8] Porto University - Faculty of Engineering, Rua Dr. Roberto Frias, s/n 4200-465 Porto, Portugal
Email : rdelgado@fe.up.pt

Usually, hollow piers have large section dimensions, with reinforcement bars spread along both wall faces. Unlike common solid section columns, quite often the shear effect has great importance on the pier behaviour. Therefore, it is of particular relevance that special attention is given to this issue when the assessment and retrofit of RC hollow section piers is envisaged. Within this framework, and in order to analyze different strategies for the seismic retrofit of RC piers, a broad testing campaign has been developing at the Laboratory of Earthquake and Structural Engineering (LESE) at the Faculty of Engineering of University of Porto (FEUP), aiming at the experimental validation of different retrofit strategies implemented on a set of RC rectangular hollow section piers. Therefore, the paper presents a brief overview of the experimental setup and its calibration, followed by the description of a test series already carried out involving a first set with the original specimens and a second set consisting of the retrofitted piers. Some results and conclusions are also presented.

2. EXPERIMENTAL CAMPAIGN

2.1. Testing setup

The test setup, shown in Fig. 1, makes use of a 500 kN actuator to apply lateral loads and a 700 kN actuator to apply axial loads. The specimen and reaction frame are bolted to the strong floor with high strength prestressed rods. A constant axial load of 250 kN was applied during the tests, herein described, while the lateral loads were cycled, under displacement controlled conditions.
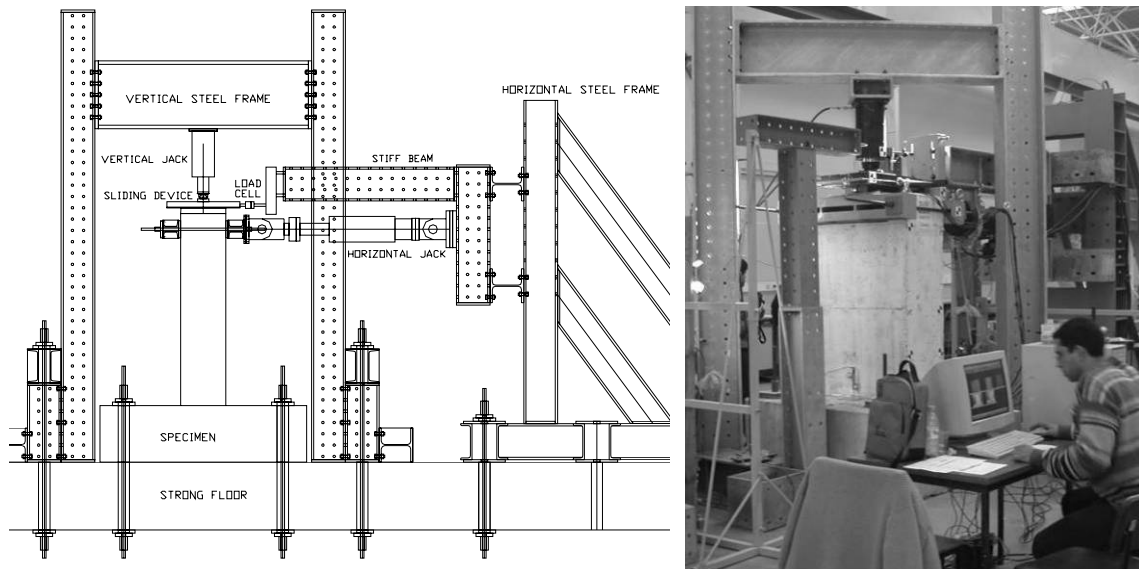

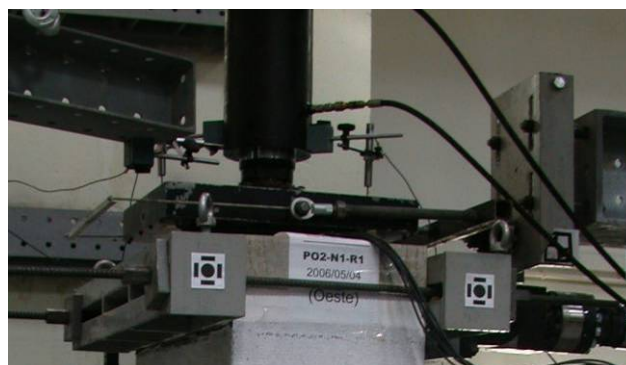**Figure 1: Schematic layout and view of the test setup at LESE laboratory.**

Figure 2: The sliding device used to apply the axial load.

A special sliding device consisting of two steel plates, shown in Fig. 2, was used to minimize the friction created by the axial loads. The lower plate is bonded to the specimen top, whereas the upper is hinged to the vertical actuator, allowing top-end displacements and rotations on the specimens to take place when lateral loading is imposed during the test. The upper plate is also connected to a load cell to measure the residual frictional force between the two plates. During the tests performed to date, an undesired problem occurred with the hydraulic

system used to apply the axial load: the pressure that should remain constant has in fact increased. Actually, the hydraulic system was designed to keep constant the oil pressure, in order to maintain constant the axial force, but a deficient performance of the circuit has blocked the oil return from the vertical actuator; therefore, the axial load increased during the cyclic displacement history, because the axial actuator was forced to remain in the same position when the top-end pier section was rotating and displacing. After this problem was eliminated, an auxiliary test to calibrate all the setup was carried out, by using a steel column hinged at the bottom, illustrated in Fig. 3, instead of the R/C specimen. The main purpose was therefore to accurately measure all the forces involved on the vertical reaction frame.
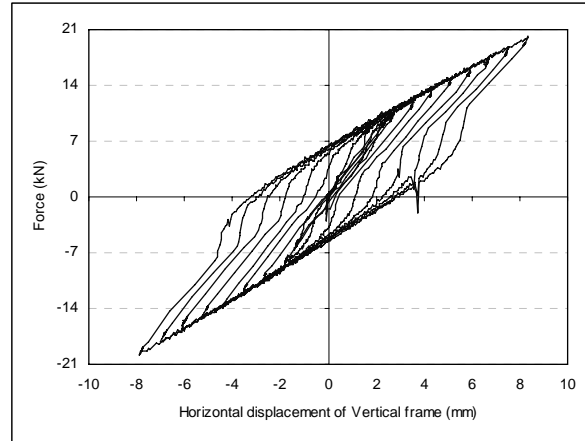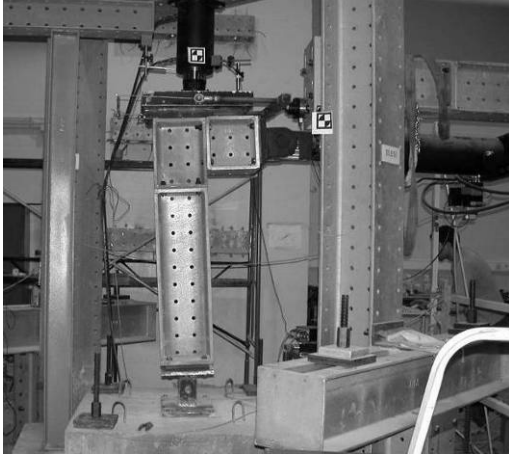

Figure 3: Setup with a steel pier hinged at the base.

Figure 4: Relationship between the horizontal force and displacement of the vertical steel frame.

Due to the column hinge the moment of all forces at the base has to be equal to zero. Thus, only three exterior forces are applied to the steel column, which produce moment at the base: the horizontal actuator force, the upper plate force (resulting from the displacement restrain at this point) and the horizontal force of the vertical reaction frame. The two first forces are measured from load cells, whereas, from the null moment equilibrium condition at the base, the horizontal force of the vertical reaction frame can be computed. Considering the same axial load, as for the real specimen piers, the diagram shown in Fig. 4 was obtained relating the aforementioned horizontal force with the horizontal displacement of the vertical frame. These results allowed determining the horizontal stiffness of the vertical reaction frame that can be used later to correct the horizontal force actually absorbed by the column. As it can be seen from the Fig. 4, two parallel lines can be defined on the hysteretic curve envelop, which correspond to the horizontal stiffness of the vertical reaction frame estimated as approximately 2.2 kN/mm. However, it is noteworthy that, probably due to the characteristics of the sliding device, a stiffness discrepancy is observed when the direction of the movement is inverted.

The actuator control is done using a PXI controller system from National Instruments (NI) and specifically home developed control routines based on the LabVIEW software platform (also from NI). The data acquisition is also based on another PXI system equipped with acquisition and signal conditioning cards and allows direct reading of data from strain gauges, load cells, LVDTs (Linear Voltage Displacement Transducers) and other types of amplified analogical or digital sensors. The data acquisition software was identically developed in LabVIEW.

2.2. Specimens and Instrumentation

This set of specimens consists of two different rectangular hollow section RC piers: the first, a 450 mm square cross section with 75mm thick walls, is similar to some piers tested at the Laboratory of Pavia University, Italy [Pavese *et al*, 2004] and the results of this specimen tests are to be compared with those obtained at Pavia; the second specimen set, a rectangular section with 450mm x 900 mm, is being tested in order to understand the influence of the cross section geometry of rectangular hollow piers on the cyclic behaviour, bearing in mind the purpose of assessing retrofitting solutions. The thickness of the pier wall was kept constant, 75 mm. The model schemes shown in Fig. 5-a correspond to ¼ scale representations of hollow section bridge piers, herein referred to as PO: PO1 for the square section and PO2 the rectangular section. Instrumentation included strain gages attached to the reinforcement bars and LVDTs to measure curvature and shear deformations along the pier height. This configuration was used in both specimens as clearly shown in Fig. 5-b where the LVDT layout is visible as used for the pier PO2. It is worth mentioning that this instrumentation layout was actually improved

from that of the first PO1 test (in which only two levels of LVDT sets were included from the pier bottom) because important shear deformations were indeed observed in that test. Therefore it became essential to distribute more LVDTs along the entire pier height as illustrated in Fig. 5-b.
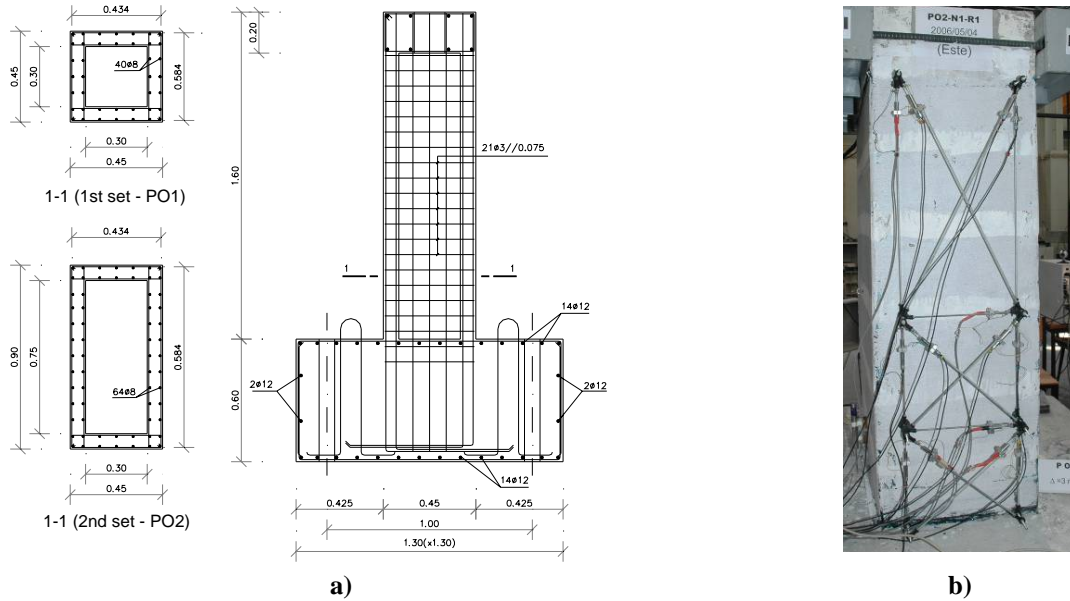

a)   b)

Figure 5: Hollow RC piers: a) model schemes and b) lateral LVDT layout for PO2

3.   CYCLIC TESTS

In order to characterize the pier cyclic behaviour, three cycles were applied for each of the following peak drift ratios: 0.1%, 0.2%, 0.35%, 0.7%, 0.3%, 1.0%, 1.2%, 0.5%, 1.8%, and 2.4%.

3.1. Pier PO1

Concerning the results of the PO1 original specimen test, little damage was observed in the north and south sides, as shown in Fig. 6 where well distributed cracks were visible. However, the damage was found strongly concentrated in the lateral sides, east and west, where the concrete cover crushed within the entire pier height. As expected, severe shear damage was observed during the test with significant concrete degradation due to the low efficiency of the transverse reinforcement.
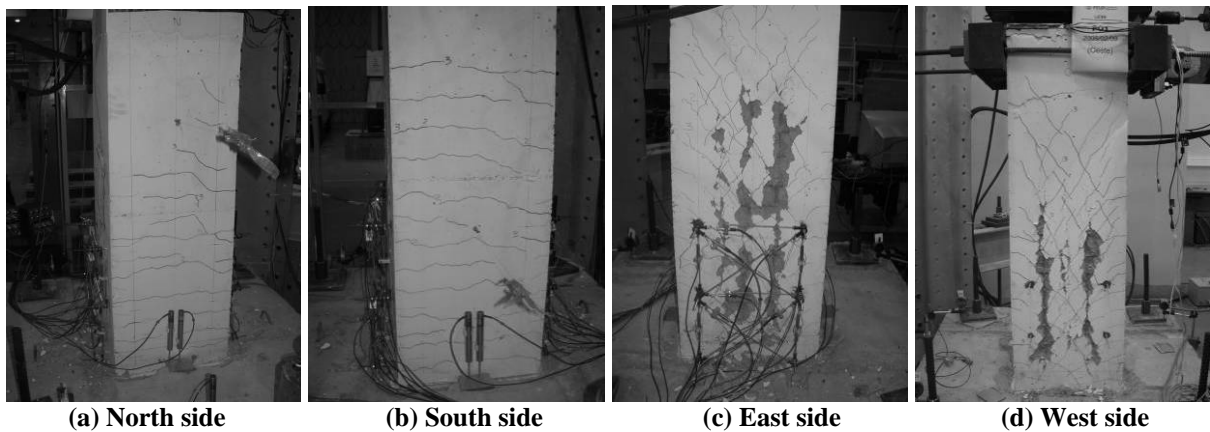

(a) North side   **(b) South side**   **(c) East side**   **(d) West side**
Figure 6: Pier PO1 damage for 2.4% drift.

3.2. Pier PO2

For the PO2 original specimen test, and as also described for the pier, the greatest amount of damage was mainly observed at the lateral sides, east and west, where the concrete cover again crushed within the entire pier height (see Fig. 7) and strong shear damage was achieved due to concrete degradation caused by lack of transverse reinforcement efficiency. Again, little damage was observed on the north and south sides, with well distributed

cracks. However, the cracks observed in those sides are not only horizontal, as for the square pier, but instead they show an angle that increases along the pier height, due the shear lag effect that occurs for this width/height ratio (2:1). Fig. 8 shows the experimental responses of both piers PO1 and PO2 where it is visible that, as expected, higher maximum forces were achieved for the rectangular section (PO2), due to the significant increase of the longitudinal reinforcement and concrete area, when compared with the square pier PO1. From the experimental responses and damage patterns illustrated in Figs. 6 and 7, shear mode failures of both piers were observed around the first cycles of 33mm amplitude (2.4% drift). However, these larger forces in the pier PO2 (only about 1,2 times those of from PO1) is not proportion with the increase of longitudinal reinforcement of pier PO2, about 2 times more when compared with pier PO1, which is related with the shear lag effect quite apparent from the damage pattern really observed.

| (a) North side | (b) South side | (c) East side | (d) West side |

Figure 7: Pier PO2 damage for 2.4% drift.
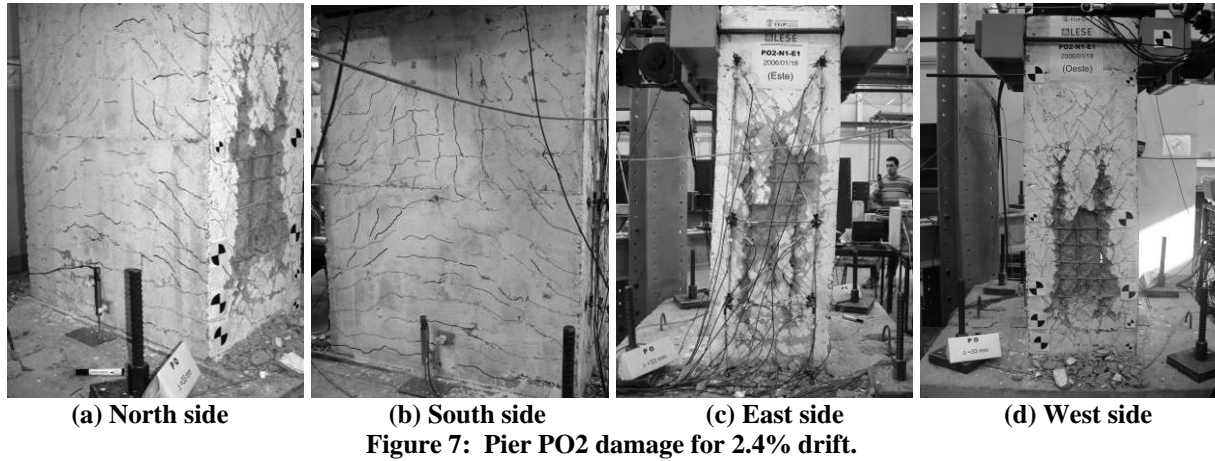
Concerning the numerical response predictions for both monotonic and cyclic loading, two analysis tools were used based on two different model types: *i)* the Seismostruct analysis program [SeismoSoft, 2004], freely on-line available in the internet, is a finite element analysis program based on the fibre modelling technique, where the inelastic behaviour spread along the member length and across the section area is explicitly simulated according to the discretization of the section into several finite area fibres (concrete and steel fibres) and of the beam-column member into several linear elements; *ii)* the CAST3M computer code [CEA, 2003], a general purpose finite element based program, where a wide variety of non-linear behaviour models are available and, particularly, the Damage model developed at FEUP [Faria *et al*, 1998] that has already proved to be suitable for seismic behaviour analysis of RC bridge piers [Faria *et al*, 2004]. The later modelling option involves: a Continuum Damage Mechanics based constitutive model for the concrete zone discretized into 2D finite elements (illustrated in Fig. 8), incorporating two independent scalar damage variables that account for the degradation induced by tensile or compressive stress conditions; the Giuffré-Menegotto-Pinto model [Giuffré and Pinto, 1970] for the cyclic behaviour simulation of the steel reinforcement discretized via truss elements; the concrete zone discretized into 2D finite elements.
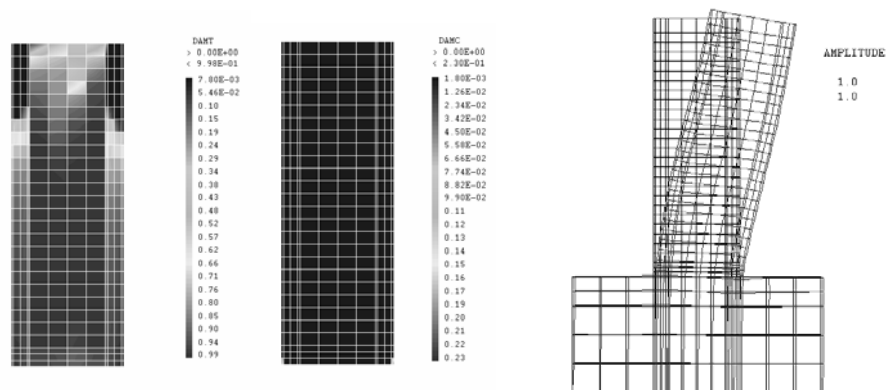

Figure 8: 2D finite element discretization with tensile/compressive damage and deformed mesh of PO1.

The simulation results with both numerical models for the pier PO1 are included in Fig. 8-a. In addition, the shear capacity curve is also depicted according to the prediction using the methodology proposed by Priestley for the shear strength [Priestley et al, 1996], and conveyed by Eq. 1:

$$V_d = V_c + V_s + V_p + V_{sj} \qquad (1)$$

where V_c, V_s and V_p are the shear force components accounting for the nominal strength of concrete, the transverse reinforcement shear resisting mechanism and the axial compression force; the term V_{sj} corresponds to the contribution of possible CFRP or metal jackets. As already referred before, the shear mechanism has significant influence on the pier response and this effect was satisfactorily captured by the damage model, for both monotonic and cyclic curves shown in Fig. 9. With the Seismostruct simulation higher maximum forces are achieved corresponding to flexural capacity of the bottom plastic hinge that, in fact, did not occur at the experimental test because it was preceded by shear mechanism. Therefore, the shear failure could not be accurately predicted by intercepting the shear capacity line, since the flexural mechanism and corresponding flexural ductility were not effectively mobilized.
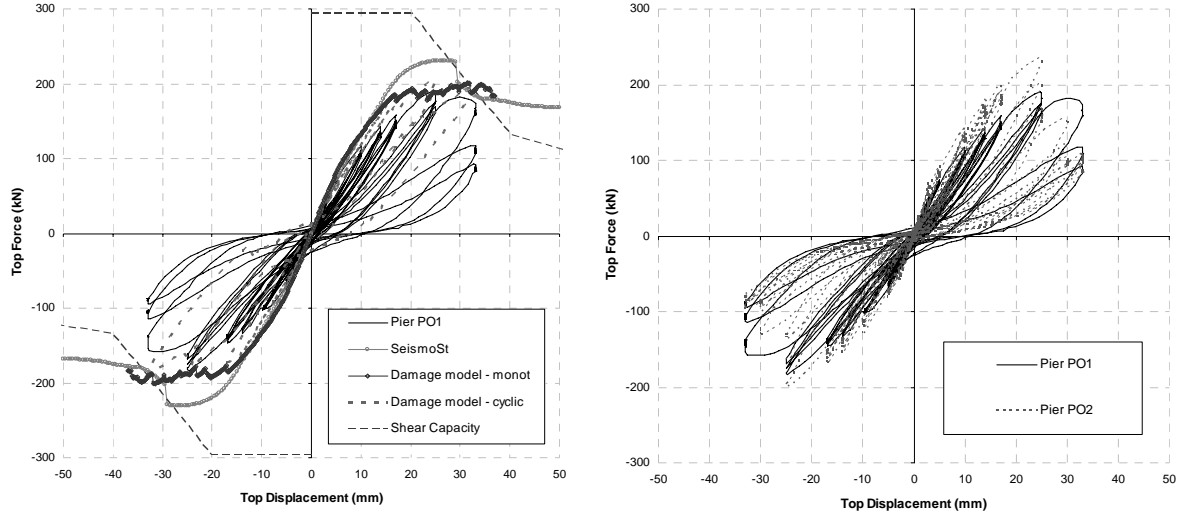

Figure 9: Numerical analysis: a) for pier PO1 and b) experimental result comparison for PO1 and PO2.

4. THE RETROFIT PROCESS

After the cyclic tests of the original specimens up to failure, they were repaired and retrofitted by an external contractor (S.T.A.P.) according to the following steps: 1) delimitation of the repair area; 2) removal and cleaning of the damaged concrete; 3) application of formwork and new concrete (Microbeton, a pre-mixed micro concrete, modified with special additives to reduce shrinkage in the plastic and hydraulic phase); 4) retrofit with the CFRP sheets. In order to provide a general idea of the pier damage and of the retrofit process, the following photographs show the piers during repair and after having been retrofitted with CFRP sheet jackets (Fig. 10).

Figure 10: Hollow piers before and after the shear retrofitting with CFRP sheet

In order to design the shear retrofit with CFRP jackets, the authors adopted the Priestley approach [Priestley *et al*, 1996] to evaluate the thickness of the rectangular hollow pier jacket for increasing the shear strength above

the maximum flexural force but keeping the initial section conditions. As seen in Eq. 1, the shear contribution of the jacketing can be included and estimated according to Eq. 2

$$V_{sj} = (A_j \, f_j \, h \cot \theta)/s = (A_j \, 0.004 E_j \, h \cot \theta)/s \tag{2}$$

where h is the overall pier section dimension parallel to the applied shear force, f_j is the adopted design jacket stress level corresponding to a jacket strain of 0.004, A_j is the transverse section area of the jacket sheets spaced at distance s and inclined of the angle θ relative to the member axis. This condition is introduced to avoid large dilation strains and hence excessive degradation of the concrete, as well as to provide adequate safety against the possibility of jacket failure. Therefore, using Eq. 1 and for the PO specimens retrofit, one layer strip of CFRP sheet of 0.117mm thickness by 100 mm width and 100 mm spaced along the height of the piers was applied, to retrofit the PO1 and PO2 specimens, as can be seen in Fig. 10.

5.   CYCLIC TEST OF THE RETROFITTED SPECIMENS

The retrofitted piers have been tested following the same cyclic displacement history of the original specimens, but two additional cycles were performed with increased top displacement amplitude corresponding to 2.9% and 3.2% peak drift ratios. Results for both specimens are included in the following sections.

5.1. Pier PO1

The damage evolution during the experimental test of the retrofitted specimen is illustrated in Fig. 11, for the east side of the pier. The first cracks, about 0.1mm wide, were visible at 0.35% drift, near the pier base. In the subsequent cycles the dimensions of theses cracks increased and new cracks were developed along the pier height (Fig. 11a). For the top displacement of 17mm (1.2% drift - Fig. 11b), only the base crack has grown to about 0.5mm. Shear cracks appeared in the next cycles of 1.8% drift and generalized damage started to become visible. In the right hand side of Fig. 11c (2.14% drift), a vertical crack is visible over almost the entire pier height, which caused global damage to the CFRP sheets. Failure of some of the fibres was audible. During the cycles of 40mm top displacement (2.9% drift - Fig. 11d) the bottom carbon sheets failed completely, leading to a drastic collapse of the pier on the compression side of the section, with buckling of the longitudinal reinforcement bars, due to lack of concrete confinement (see also Fig. 12). From these damage illustrations it can be seen that the retrofitted specimen showed a good behaviour in comparison with the original configuration, exhibiting very distributed cracking along the CFRP spacing.

The shear retrofit design used on this pier, showed an excellent performance because the shear failure mechanism was partially prevented and the flexural collapse with buckling of the reinforcement bars was achieved. In Fig. 13 the comparison between the original and retrofitted pier is illustrated, where increases can be found of 30% for the top force and of 30% for the maximum displacement reached without significant reduction of the resistant force.
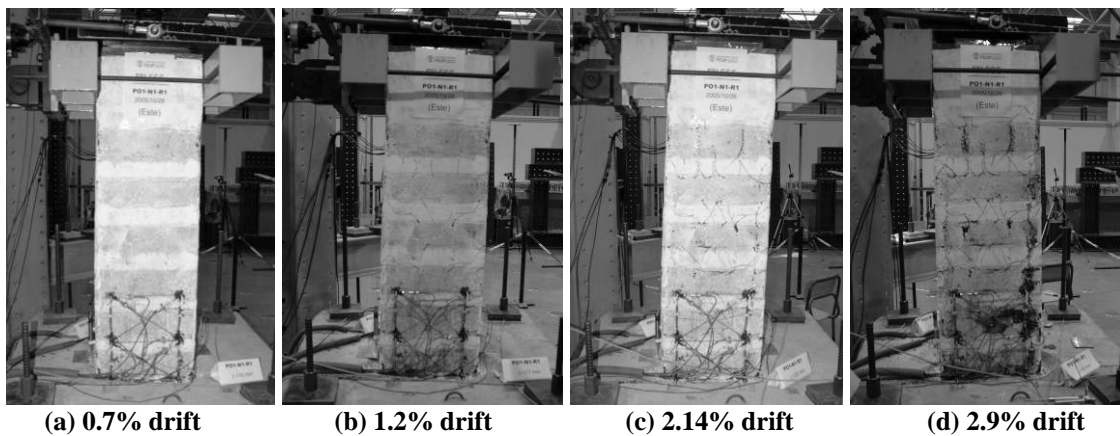

| (a) 0.7% drift | (b) 1.2% drift | (c) 2.14% drift | (d) 2.9% drift |

Figure 11: Retrofitted pier PO1 damage from east side view.

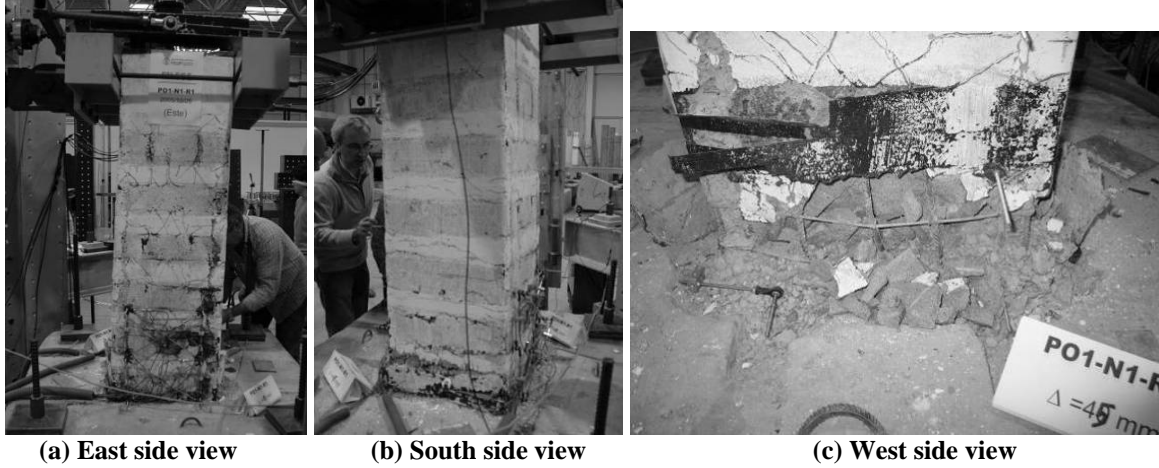| (a) East side view | (b) South side view | (c) West side view |

Figure 11: Final damage of the retrofitted pier PO1 corresponding to 3.2% drift ratio.
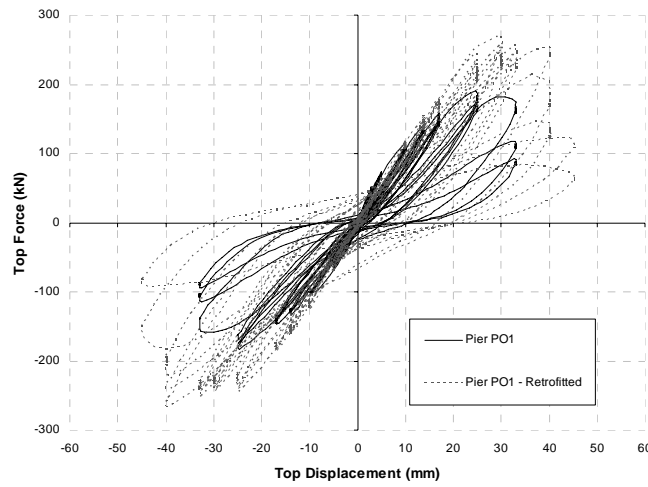

Figure 13: Experimental results of pier PO1 before and after retrofit.

5.2. Pier PO2

The damage evolution during the experimental test of the retrofitted specimen PO2 is illustrated in Fig. 14, for the pier west side. For small amplitude cycles, corresponding to drift below 0.7%, first cracks about 0.1mm wide occurred at the pier base section (Fig. 14a). In the subsequent cycles the crack widths increased and new cracks were also developed along the pier height. For the top displacement of 17mm (1.2% drift), the damage pattern shown in Fig. 14b was mainly characterized by diagonal cracks in the interval zones between the CFRP strips. Shear damage continued to increase in the next cycles and, for 2.14% drift, (Fig. 14c) some small damage started to become visible on the CFRP sheets. Failure of some of the fibres was audible from this stage on. During the last cycles of 33mm top displacement (2.4% drift) some of the carbon sheets failed completely; however, probably due to some non-symmetric conditions of the pier, more damage was found in the west side. In fact, three CFRP strips collapsed in the pier west face (shown in Fig. 14d) and only one failed at the opposite side, leading to conclude that, at the retrofit stage, the CFRP sheet bonding on the pier faces was well performed and the rupture of one side does not produce the all strip fibre failure. Fig. 15 shows the damage evolution on the pier internal faces also visualized during the test, in correspondence with the exterior damage, presented in Fig. 14. When the first CFRP strips collapsed, for 2.4% drift, the interior cracks increased considerably, as illustrated in Fig. 15d. On the last cycles, generalized damage became visible, with almost all the CFRP strips collapsed (Fig. 16) and a quick reduction of the pier capacity was observed (Fig. 17). The final interior damage is also shown in Fig. 16d. As can be seen in Figs. 14 and 17, the retrofitted specimen showed good behaviour in comparison with the original one, exhibiting very distributed cracking along the CFRP spacing. The shear retrofit design, used for this pier, showed excellent performance since the shear failure mechanism was partially prevented and the collapse was achieved after the CFRP failed, what occurs further after the original specimen. Fig. 17 shows the comparison between the original and retrofitted pier, where about 40% increase of the top force is reached and about 50% more of the maximum displacement is obtained, without significant reduction of the resistant force.
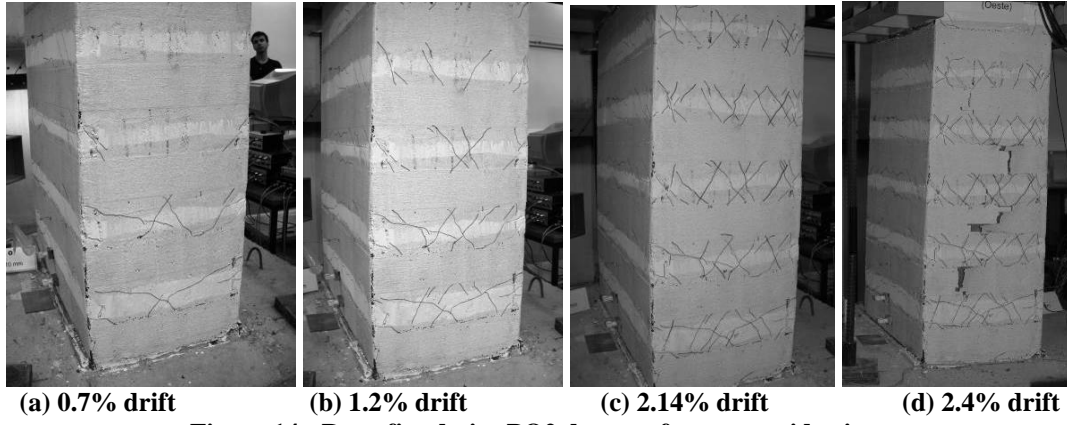
| (a) 0.7% drift | (b) 1.2% drift | (c) 2.14% drift | (d) 2.4% drift |

Figure 14: Retrofitted pier PO2 damage from west side view.

| (a) 0.7% drift | (b) 1.2% drift | (c) 2.14% drift | (d) 2.4% drift |
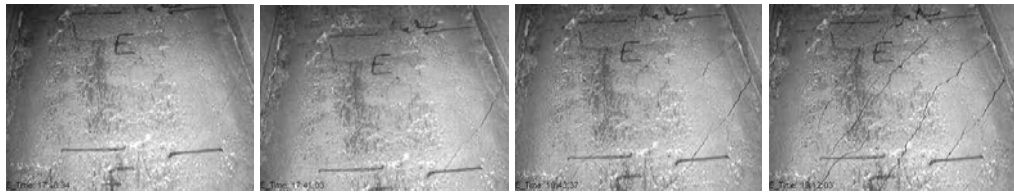
Figure 15: Retrofitted pier PO2 damage from internal east side view.

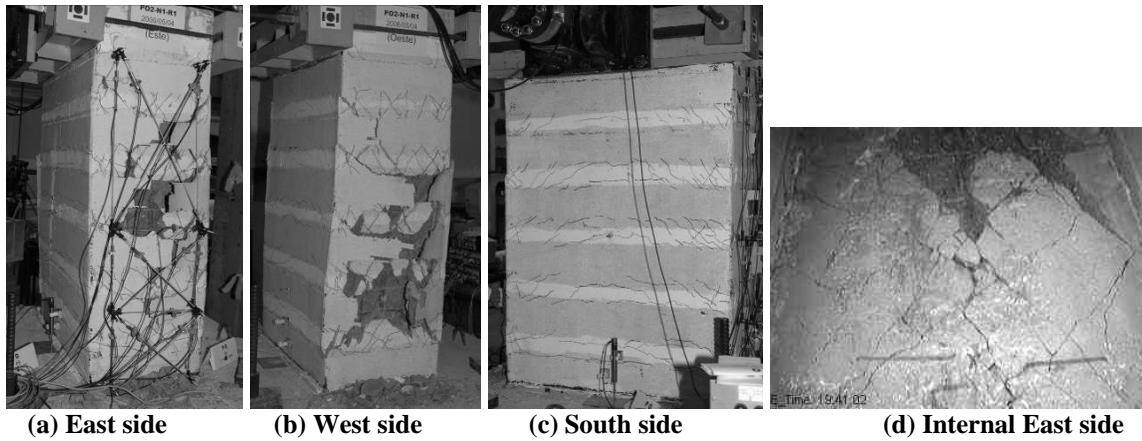| (a) East side | (b) West side | (c) South side | (d) Internal East side |

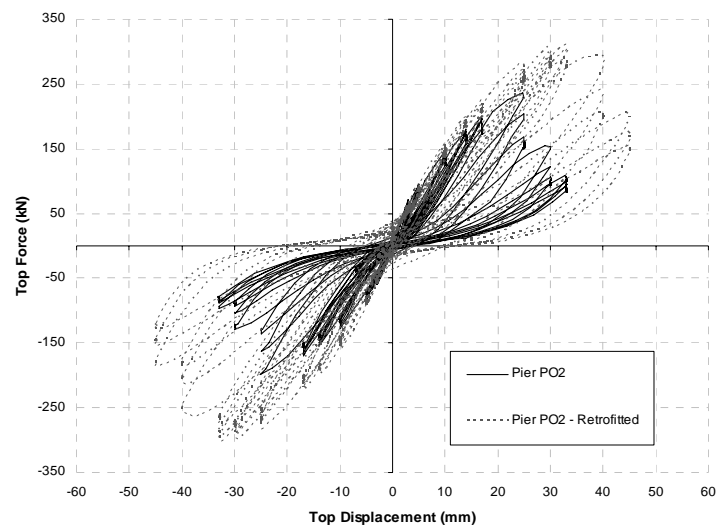**Figure 16: Final damage views of the retrofitted pier PO2 corresponding to 3.2% drift ratio.**

Figure 17: Experimental results of pier PO2 before and after retrofit.

6. CONCLUSIONS

An experimental setup was presented for cyclic tests of piers, keeping the position and intensity of the axial load during the cyclic movement, by means of a sliding device to allow top displacements of the pier. A calibration test using a pinned steel column was described and the procedure for the evaluation of the actual column horizontal force was also addressed. This test and subsequent ones evidenced satisfactory performance of the setup with low values of frictional forces that can be measured and considered on the final results.

The PO1 and PO2 original specimen tests evidenced that the collapse was achieved because of insufficient shear capacity. In both tests cracks were observed at lateral sides (east and west faces), where the concrete cover crushed within the entire pier height and severe shear damage was observed with significant concrete degradation due lack of transverse reinforcement efficiency. For the PO2 pier, the shear lag effect was also observed as evidenced by inclined cracks at the North and South sides, and the consequent reduction of the maximum predicable top horizontal force.

The numerical solution obtained with the accurate method, the damage model, agrees very well with the experimental results; besides for the seismostruct model a little higher results were obtained, because the non linear effects due to the shear forces were not included.

The CFRP retrofit showed excellent benefits on the two piers behaviour since it avoided the shear collapse and a mixed shear-flexure mechanism was achieved. The ultimate drift increased from 2.4% to 3.2%%, on both piers, and a well distributed cracking was obtained. The adopted retrofitting strategy has evidenced good ability for the improvement of the seismic pier behaviour both in ductility and strength. The retrofitting of the PO2 pier evidenced a higher improvement on the horizontal force capacity than the PO1, due the benefits of the CFRP retrofit, both in shear strength and in the shear lag effect, allowing a great participation of the tensile wall of the pier.

7. ACKNOWLEDGMENTS

8. REFERENCES

Delgado, P.; Costa, A. and Delgado, R. (2004), Different Strategies for Seismic Assessment of Bridges – Comparative studies. *Proceedings of the 13th World Conference on Earthquake Engineering*, August 1-6. Vancouver, Canada: *Paper N. 1609*.

Delgado, P.; Rodrigues, V.; Rocha, P.; Arêde, A.; Pouca, N.; Costa, A. and Delgado, R. (2006), Experimental Tests on Seismic Retrofit of RC Piers. *100th Anniversary Earthquake Conference*, April 18-22. San Francisco, USA: *Paper N. 1688*.

Faria, R., Oliver, J. and Cervera, M. (1998), A strain-based plastic viscous-damage model for massive concrete structures. *International Journal of Solids and Structures*, 35(14), 1533-1558.

Faria, R., Pouca, N. and Delgado, R. (2004), Simulation of the cyclic behaviour of R/C rectangular hollow section bridge piers via a detailed numerical model. *Journal of Earthquake Engineering*, Vol. 8, No. 5 725-748.

Giuffrè, A. and Pinto, P. (1970), Il comportamento del cemento armato per sollecitazione ciclice di forte intensitá, *Giornale del Genio Civile*.

Pavese, A.; Bolobnini D. and Peloso S. (2004), FRP Seismic Retrofit of RC Square Hollow Section Bridge Piers. *Journal of Earthquake Engineering*, 8, Special Issue 1, 1–26, Imperial College Press

Priestley, M. J. N.; Seible, F. and Calvi, G. M. (1996), Seismic Design and Retrofit of Bridges. *John Wiley & Sons,* New York.

Rocha, P.; Delgado, P.; Costa, A. and Delgado, R. (2004), Seismic retrofit of RC frames, Computers & Structures, 82, 1523-1534. Elsevier.

SeismoSoft 2004. SeismoStruct - A computer program for static and dynamic nonlinear analysis of framed structures [online]. Available at: http://www.seismosoft.com.